Letter

Tunable critical field in Rashba superconductor thin films

L. A. B. Olde Olthof [●],[*] J. R. Weggemans [●], G. Kimbell [●], J. W. A. Robinson [●],[†] and X. Montiel [●][‡]

Department of Materials Science & Metallurgy, University of Cambridge, CB3 0FS Cambridge, United Kingdom

Strong intrinsic or interfacial spin-orbit coupling (SOC) can enable a thin-film superconductor to exceed the paramagnetic limit. For Rashba-type SOC, we show that the superconducting thermodynamic properties of a finite-size thin film are strongly sample-size dependent due to the creation of edge states; for example, in the case of geometrically anisotropic thin films, the critical field is found to be tunable through the direction of an externally applied in-plane magnetic field. These findings open perspectives for the development of superconducting spin-orbitronic devices.

Spin-singlet *s*-wave superconductivity is destroyed by a magnetic field via orbital [1] or Pauli paramagnetic effects [2,3]. In superconducting thin films, the orbital contribution is negligible for in-plane magnetic fields [4] and spin-singlet pairs are destroyed when the Zeeman splitting energy exceeds the binding energy of a pair, defining the upper critical field h_p (i.e., the Clogston-Chandraskhar or Pauli paramagnetic limit [2,3]).

Several methods have been explored to overcome h_p. In clean superconductors, spin-singlet pairs acquire a finite momentum under an applied magnetic field with a spatially modulated pair wave function described by the Larkin-Ovchinnikov-Fulde-Ferrell (LOFF) state, which increases h_p [5–9]. Enhancements of h_p have been observed in the presence of spin-orbit scattering, which randomizes spins that scatter off boundaries [10] or impurities [11–14]. Recently, enhancement of h_p has been demonstrated in Ising superconductors where spin-orbit coupling (SOC) induces an effective Zeeman field that pins electron pair spins out of plane so they are insensitive to in-plane applied magnetic fields [15–29]. Theoretical studies have highlighted the possibility to affect superconducting properties via SOC in singlet [30] and triplet superconductors [31]. Tuning of the superconducting order parameter has been proposed in nonlocal devices via nonequilibrium potentials [32] or in one-dimensional Rashba superconductors using different geometries such as curved wires and ring structures [33,34].

In this letter, we theoretically investigate the effect of Rashba SOC-induced anisotropy (Fig. 1) on the magnetic field-temperature (h, T) phase diagram of a finite-sized thin-film *s*-wave superconductor. We show that the Rashba SOC leads to a significant enhancement and geometric dependence of the paramagnetic limit. In particular, we demonstrate that h_p is controllable through the direction of an externally

applied in-plane magnetic field in geometrically anisotropic superconducting thin films at equilibrium.

The usual quadratic dispersion is split into two helicity bands with energies $E_\pm = \hbar k^2/2m \pm \alpha|k|$, where α is the SOC strength and k the single-particle momentum [35]. The spins are polarized tangential to their momentum as illustrated in Fig. 1(b). For each direction in momentum space, there are two zero-momentum opposite-spin pairs on the Fermi surface. With an in-plane magnetic field $\vec{h} = (h_x, h_y, 0)$, the dispersion becomes $E_\pm = \hbar k^2/2m \pm \sqrt{(\alpha k_y + h_x)^2 + (\alpha k_x - h_y)^2}$ [35]. The Fermi surfaces shift in the direction perpendicular to the magnetic field, producing an intrinsic spatial anisotropy [see Fig. 1(c)]. Consequently, the singlet pairs acquire a net momentum and a LOFF-like state forms in the clean limit [36–38]. The critical field experiences a sharp
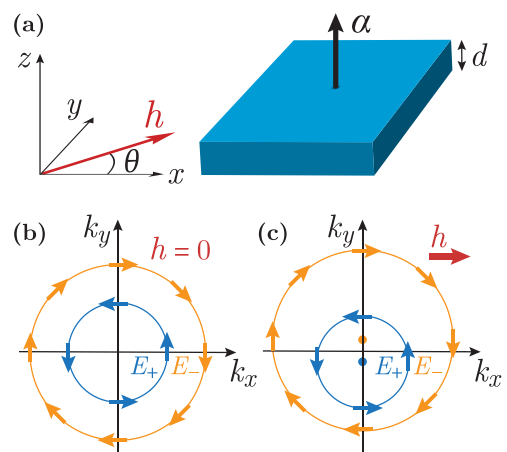
FIG. 1. (a) Schematic illustration of a thin-film superconductor with thickness d and out-of-plane spin-orbit coupling $\vec{\alpha}$ in an externally applied in-plane magnetic field $\vec{h}$. (b) Fermi surface of a Rashba superconductor with spins locked to the momentum, forming two helicity bands E_+ and E_-. (c) The magnetic field $\vec{h} = (h_x, 0, 0)$ shifts the helicity bands vertically (the dots represent their new centers). In a magnetic field, the Rashba superconductor has intrinsic spatial anisotropy.

[*]labo2@cam.ac.uk
[†]jjr33@cam.ac.uk
[‡]xm252@cam.ac.uk

incline at low temperatures, surpassing the paramagnetic limit [37,39]. In the diffusive regime, the LOFF-like state disappears and a spatially modulated helical state remains [39,40] that is stable against disorder since it originates from the SOC symmetry [41]. Disordered Rasbha superconductors with strong SOC in an in-plane magnetic field thus have an enhanced critical field [39,40] and critical temperature [42].

We investigate superconducting thin films with in-plane magnetic field $\vec{h}$ (externally applied or via an induced exchange field). We model superconductivity in the diffusive limit via the Usadel formalism, which is formulated in terms of Green's functions [43]. The Green's functions $\hat{g}(\vec{R}, \omega_n)$ depend on the spatial center-of-mass coordinate $\vec{R}$ and the Matsubara frequencies $\omega_n = (2n + 1)\pi T$ (T is the temperature and $n \in \mathbb{Z}$); in $4 \otimes 4$ spin $\otimes$ particle-hole space, $\hat{g}(\vec{R}, \omega_n)$ is expressed as [43]

$$\hat{g} = \begin{pmatrix} g & f \\ \tilde{f} & \tilde{g} \end{pmatrix}, \tag{1}$$

where g and f are the normal and anomalous Green's functions, respectively, and $\tilde{g}$ and $\tilde{f}$ are their particle-hole conjugates [43]. In the diffusive limit, the Green's functions satisfy the Usadel transport equation [43],

$$[i\omega_n \hat{\tau}_z - \hat{\Delta} - \vec{h} \cdot \vec{\sigma}, \hat{g}] + \frac{D}{\pi} \nabla(\hat{g}\nabla\hat{g}) = 0, \tag{2}$$

with the normalization condition $\hat{g}^2 = -\pi^2 \hat{1}$. In Eq. (2), $\vec{\sigma}$ and $\vec{\tau}$ are the Pauli matrices in spin and particle-hole space, respectively, D is the diffusion coefficient, and $\hat{\Delta} = \Delta_s i\sigma^y$ is the conventional superconducting order parameter. The Rashba SOC gives rise to an effective momentum-dependent exchange field, i.e., the spin-orbit field. To include this in the Usadel equations, we introduce the covariant derivative $\bar{\nabla} \mapsto \nabla - i[\underline{\hat{A}}, .]$, where ∇ is the standard derivative and $\underline{\hat{A}}$ the spin-orbit field vector [44–46]. In the following, we assume that the spin-charge conversion terms are negligible [47]. Close to the critical temperature T_c, the Usadel equations become [43]

$$(D\bar{\nabla}^2 - 2|\omega_n|)f_s = -2\pi \Delta_s + 2i \, \mathrm{sgn}(\omega_n)\vec{h} \cdot \vec{f}_t$$
$$(D\bar{\nabla}^2 - 2|\omega_n|)\vec{f}_t = 2i \, \mathrm{sgn}(\omega_n)\vec{h}f_s, \tag{3}$$

where the normal Green's function is $\hat{g} = -i\pi\hat{\tau}_z$ and the anomalous Green's function is decomposed in the spin Pauli matrices base as $f = (f_s + \vec{f}_t \cdot \vec{\sigma})i\sigma^y$, where f_s is the singlet correlation and $\vec{f}_t = (f_t^x, \ f_t^t, \ f_t^z)^T$ the triplet correlation.

In the following, we study superconducting thin-films lying in the xy-plane with thickness d smaller than the superconducting coherence length, i.e., $d \leqslant \xi$, with $\xi = \sqrt{D/2\pi T_{c0}}$. We assume that the superconductivity is uniform in z, such that the Green's functions only depend on the x and y coordinates, i.e., $\hat{g}(\vec{R}, \omega_n) = \hat{g}(x, y, \omega_n)$. The spin-orbit field is $\vec{\alpha} = \alpha(\vec{s} \times \vec{p}) \cdot \hat{n}$, where α is the SOC strength (in units of $1/\xi$), the spin $\vec{s} = |\vec{h}|(\cos\theta, \ \sin\theta, \ 0)^T$ is determined by the in-plane field $\vec{h}$ [see Fig. 1(a)], the momentum in a thin film is $\vec{p} = (p_x, \ p_y, \ 0)^T$ and the unit vector along the axis of broken symmetry is $\hat{n} = \hat{z}$. Hence, the spin-orbit field becomes $\vec{\alpha} = \alpha(h_x p_y - h_y p_x)\hat{z}$ and is directed out-of-plane. The corresponding spin-orbit field coefficients in spin space are

(a) $\frac{h}{T_{c0}}$
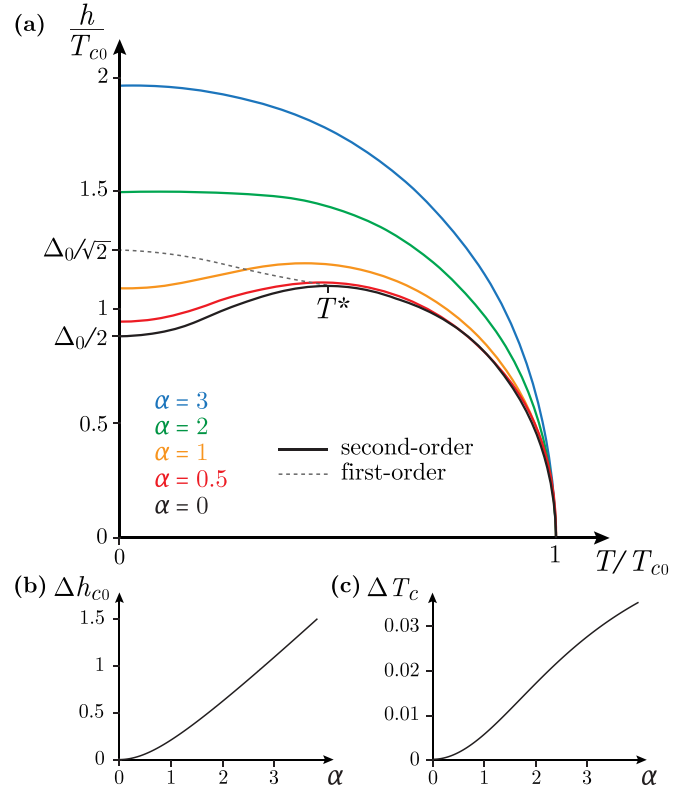
FIG. 2. Properties of an infinite thin-film Rashba superconductor. (a) Phase diagram for different values of Rashba spin-orbit coupling strength α. Solid lines are second-order self-consistent transitions, meaning that the order parameter vanishes at $\Delta(T = T_c) = 0$. The dashed line is the first-order paramagnetic limit at $\alpha = 0$. Both phase transition lines meet at the tricritical point at $T = T^*$ [49]. For $T < T^*$, the second-order phase transition defines the supercooling magnetic field. (b) The increase in critical field at zero temperature $\Delta h_{c0} = |h_{c0}(\alpha) - h_{c0}(\alpha = 0)|/T_{c0}$ with α. (c) The increase in critical temperature $\Delta T_c = |T_c(\alpha) - T_c(\alpha = 0)|/T_{c0}$ with α, for fixed applied field $h/T_{c0} = 0.5$.

$A_x = -\alpha\sigma^y$, $A_y = \alpha\sigma^x$ and $A_z = 0$, which are used in the covariant derivative $\bar{\nabla}$ (see Ref. ([48] S1) for details).

We first investigate the (h, T) phase diagram for an infinite in (x, y) thin-film Rashba superconductors. In infinite films, the spatial derivative in Eq. (3) can be neglected. We derive the self-consistency equation and solve it analytically ([48] S5) to map the phase diagram in Fig. 2(a). With increasing SOC strength α, the critical field increases and the transition takes on a concave shape, similar to Ref. [39]. The spin-momentum locking caused by SOC renormalizes the magnetic field, meaning that with increasing α, the effective $\vec{h}$ decreases ([48] S5). At zero magnetic field, SOC does not affect T_c, showing that SOC does not affect the superconductivity but screens the applied magnetic field [50]. A similar screening effect is observed in the presence of spin-orbit scattering in disordered superconductors [12,14].

SOC increases the critical field, as shown at zero temperature in Fig. 2(b). The magnitude of ΔT_c at finite magnetic field, seen in Fig. 2(c), is similar to the temperature recovery predicted in superconductor/ferromagnet bilayers [51]. We note that the largest change in h_{c2} is two orders of magnitude

higher than the change in T_c, implying that the effect of SOC on magnetic field is more easily observable.

While the SOC screens the magnetic field in infinite thin films, an additional effect appears at the edge of finite samples. Edge states with distinct physical properties from the infinite film superconductors may appear similar to topological superconductors [52,53]. We consider a finite $L_x \times L_y$ superconductor, where L_x and L_y are in units of ξ. The spin current cannot leave the sample, meaning that its component perpendicular to the edges is zero [44,53]. Since the spin current is proportional to the covariant derivative, the latter is also zero at the edges, such that ([48] S3)

$$\partial_i f_s|_{i=0,L_i} = 0,$$
$$\partial_i f_t^x\big|_{i=0,L_i} + 2\tilde{\alpha} f_t^z \delta_{ix} = 0,$$
$$\partial_i f_t^y\big|_{i=0,L_i} + 2\tilde{\alpha} f_t^z \delta_{iy} = 0,$$
$$\partial_i f_t^z\big|_{i=0,L_i} - 2\tilde{\alpha} f_t^i = 0, \qquad (4)$$

with $i = x, y$ and δ_{ij} the Kronecker delta. Using these boundary conditions, we calculate the phase diagram iteratively, starting from the analytical infinite film solution as an ansatz ([48] S6).

The numerical phase diagram for a $L \times L$ superconductor is shown in Fig. 3(a). Since L is in units of ξ, $L = 20$ converges to the analytical infinite film solution. Decreasing L reduces h_{c2} compared to the corresponding infinite film value.

The presence of triplet correlations $\vec{f}_t$ induces a spin magnetization in the superconducting film defined as [54]

$$\vec{M}(x, y) = (M_x, M_y, M_z) = M_0 \frac{T}{T_{c0}} \sum_n f_s \vec{f}_t, \qquad (5)$$

where M_0 is a constant defined in Ref. ([48] S7) and the summation is over the Matsubara frequencies. The boundary conditions Eq. (4) couple in-plane triplet correlations f_t^x and f_t^y to out-of-plane triplet correlations f_t^z. Under an applied field $\vec{h} = (h_x, 0, 0)$, this results in an out-of-plane magnetization M_z at the edges transverse to $\vec{h}$ [53]. The resulting magnetization profile is positive on one side of the sample, zero in the middle, and negative on the other side [53], as shown in Figs. 3(b) and 3(c). The magnetization acquires this profile in the field direction (along x) while remaining nearly constant in the perpendicular direction (along y). For small L, a magnetization gradient spans the whole sample. Upon increasing L, the magnetization becomes concentrated at the edges. A similar effect is seen when increasing α. The profile resembles that of the spin-orbit induced local magnetic field in a superconductor/ferromagnet bilayer and could therefore lead to the formation of vortices [51].

When the system becomes small ($L \sim \xi$) [55], the edges dominate the sample properties and we recover the infinite film phase diagram in the absence of SOC ([48] S4), as seen in Fig. 3(a). This means that the edge effect cancels the enhancement of h_{c2} from the screening effect in infinite films. We thus conclude that the SOC gives rise to two competing effects: the infinite film screening effect (increasing h_{c2}) and the edge effect (suppressing h_{c2}).

The critical field h_{c0} and magnetization M_z are shown as a function of L for different values of α in Figs. 3(d) and 3(e). For $L \sim \xi$, the edge effect dominates and h_{c0} and M_z rapidly increase with L. For large L, h_{c0} saturates and M_z gradually
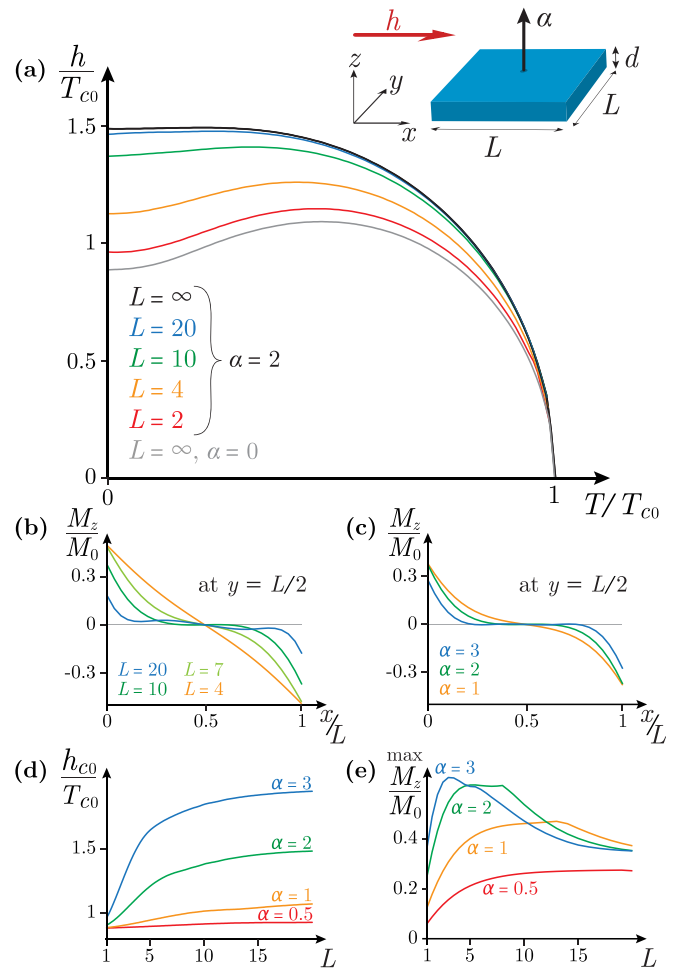
FIG. 3. The effect of finite size. Top-right inset: Geometrically constrained $L \times L$ thin-film superconductor with out-of-plane spin-orbit coupling $\vec{\alpha}$ in an applied magnetic field $\vec{h} = (h_x, 0, 0)$. (a) Phase diagram of a $L \times L$ superconductor with $\alpha = 2$ (colored), along with the analytical infinite film solutions for $\alpha = 2$ (black) and $\alpha = 0$ (grey). (b) The profile of the induced out-of-plane spin magnetization M_z in the field direction (along x) in the middle of the sample ($y = L/2$) for fixed $\alpha = 2$ and different values of L. (c) The same profile for fixed $L = 10$ and different values of α. (d) The critical field at zero temperature h_{c0} and (e) the maximum of M_z as a function of L, for different values of α.

drops off to a residual magnetization which is not present in infinite films (in which $M_z = 0$). However, this residual magnetization no longer affects the thermodynamic properties which become similar to the infinite film [see Fig. 3(a)].

To investigate further the edge effect, we calculate the phase diagram of a rectangular superconductor with $L_x > L_y$. The shape anisotropy introduces an in-plane angle θ between $\vec{h}$ and the x axis [see Fig. 1(a)]. When $\vec{h}$ points along the larger dimension ($\theta = 0$), the edge magnetization M_z is concentrated along the shorter dimension [see Fig. 4(b)]. It covers only a small part of the sample resulting in a slight suppression of h_{c2}. Upon rotating θ, M_z becomes more widely distributed over the sample, resulting in further suppression of h_{c2}. Finally, when $\vec{h}$ is along the short dimension ($\theta = \pi/2$),

(a)

(b) $\theta = 0$

$\theta = \pi/4$

$\theta = \pi/2$

$\frac{M_z}{M_0}$

(c) h_{c0}

$L_x = 10$

(d) h_{c0}

$L_x \to \infty$
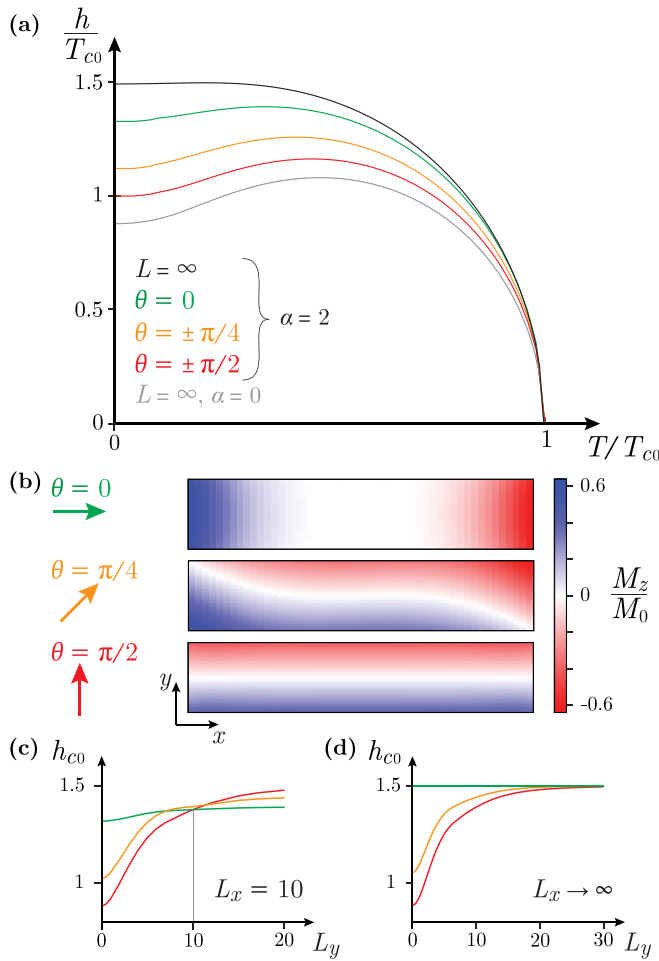
FIG. 4. The effect of shape anisotropy. (a) Phase diagram of a rectangular superconductor with $\alpha = 2$, $L_x = 5L_y$, along with infinite film solutions for $\alpha = 2$ (black) and $\alpha = 0$ (grey). (b) Corresponding spatial distribution of the out-of-plane magnetization M_z. (c) The effect of anisotropy on the critical field h_{c0}. (d) The one-dimensional limit.

M_z affects most of the film and h_{c2} reaches a minimum, approaching again the infinite film in the absence of SOC [see Fig. 4(a)]. This shows that h_{c2} is controllable by sample geometry in combination with the applied field direction.

The quantitative effect of the field direction on a superconductor with constant L_x and increasing L_y is shown in Fig. 4(c). When the field is along L_x ($\theta = 0$), h_{c0} is nearly constant, except for a slight decrease for small L_y corresponding to the overall size suppression. The $\theta = 0$ and $\theta = \pm\pi/2$ graphs intersect for $L_x = L_y$. Upon increasing $L_y > L_x$, the $\theta = \pm\pi/2$ direction becomes favorable. In this regime, the difference between the angles is less severe, since the size suppression is small.

In narrow superconducting strips with $L_x \gg L_y$, the system becomes effectively one-dimensional. The limit where $L_x \to \infty$ and L_y remains finite is shown in Fig. 4(d). When the field is along the infinite direction, h_{c0} equals the infinite film limit, which confirms that any suppression of h_{c0} (compared to the infinite film) is a result of finite size. This implies that, experimentally, the effect of SOC can be turned on and off in a narrow strip by rotating the in-plane field. In the same limit, we compare the quasiclassical model presented here to an existing Ginzburg-Landau model [51]. The angular dependency of the phase diagram close to T_c can be recovered from thermodynamic arguments ([48] S8), supporting the results presented here. Since our calculation is in the diffusive limit (i.e., mean-free path $\lambda \ll \xi$), we expect our results to be valid when $L, L_x, L_y \gtrsim \xi$.

We have shown that the paramagnetic limit h_p of a thin-film superconductor is enhanced by Rashba SOC and that tunable superconductivity is achieved using three parameters: the SOC strength, the sample geometry, and the applied field direction. In shape anisotropic samples, the critical field is changed by rotating the magnetic field for the entire temperature range up to T_c. The ability to control superconductivity using SOC opens possibilities for superconducting spin-orbitronics devices.

A possible experimental setup is an s-wave superconducting thin-film/heavy-metal bilayer with a bilayer thickness within ξ), such as Nb/Pt. This can be extended to heterostructures with ferromagnets (e.g., Nb/Pt/Co) in which h_{c2} is controlled by the ferromagnetic exchange field. Alternatively, to control the SOC within a single sample, the superconductor can be coupled to a two-dimensional chalcogenide in which the SOC is tuned by gating [56,57].

[1] P. De Gennes, *Superconductivity of Metals and Alloys* (Westview Press, United States, 1966).

[2] A. M. Clogston, Phys. Rev. Lett. **9**, 266 (1962).

[3] B. Chandrasekhar, Appl. Phys. Lett. **1**, 7 (1962).

[4] M. Tinkham, *Introduction to Superconductivity* (Dover Publications, United States, 1996).

[5] A. I. Larkin and Y. N. Ovchinnikov, Zh. Eskp. Teor. Fiz. **47**, 1136 (1964) [J. Exp. Theor. Phys. **20**, 762 (1965)].

[6] P. Fulde and R. A. Ferrell, Phys. Rev. **135**, A550 (1964).

[7] Y. Matsuda and H. Shimahara, J. Phys. Soc. Jpn. **76**, 051005 (2007).

[8] L. G. Aslamazov, J. Exp. Theor. Phys. **28**, 773 (1969).

[9] L. N. Bulaevskii and A. A. Guseinov, Sov. J. Low Temp. Phys. **2**, 140 (1976).

[10] R. A. Ferrell, Phys. Rev. Lett. **3**, 262 (1959).

[11] P. W. Anderson, Phys. Rev. Lett. **3**, 325 (1959).

[12] A. A. Abrikosov and L. P. Gor'kov, J. Exp. Theor. Phys **15**, 752 (1962).

[13] R. A. Klemm, A. Luther, and M. R. Beasley, Phys. Rev. B **12**, 877 (1975).

[14] C. Grimaldi, J. Phys.: Condens. Matter **12**, 1329 (2000).

[15] Y. Saito, T. Nojima, and Y. Iwasa, Nat. Rev. Mater. **2**, 16094 (2017).

[16] Y. Saito, Y. Kasahara, J. Ye, Y. Isawa, and T. Nojima, Science **350**, 409 (2015).

[17] Y. Xing, H.-M. Zhang, H.-L. Fu, H. Liu, Y. Sun, J.-P. Peng, F. Wang, X. Lin, X.-C. Ma, Q.-K. Xue, J. Wang, and X. Xie, Science **350**, 542 (2015).

[18] Y. Liu, Z. Wang, X. Zhang, C. Liu, Y. Liu, Z. Zhou, J. Wang, Q. Wang, Y. Liu, C. Xi, M. Tian, H. Liu, J. Feng, X. C. Xie, and J. Wang, Phys. Rev. X **8**, 021002 (2018).

[19] J. Lu, O. Zheliuk, Q. Chen, I. Leermakers, N. E. Hussey, U. Zeitler, and J. Ye, Proc. Natl. Acad. Sci. USA **115**, 3551 (2018).

[20] Y. Xu, B. Yan, H.-J. Zhang, J. Wang, G. Xu, P. Tang, W. Duan, and S.-C. Zhang, Phys. Rev. Lett. **111**, 136804 (2013).

[21] M. Liao, Y. Zang, Z. Guan, H. Li, Y. Gong, K. Zhu, X.-P. Hu, D. Zhang, Y. Xu, Y.-Y. Wang, K. He, X.-C. Ma, S.-C. Zhang, and Q.-K. Xue, Nat. Phys. **14**, 344 (2018).

[22] Y. Liu, Y. Xu, J. Sun, C. Liu, Y. Liu, C. Wang, Z. Zhang, K. Gu, Y. Tang, C. Ding, H. Liu, H. Yao, X. Lin, L. Wang, Q.-K. Xue, and J. Wang, Nano Lett. **20**, 5728 (2020).

[23] J. Lu, O. Zheliuk, I. Leermakers, N. Yuan, U. Zeitler, K. Law, and J. Ye, Science **350**, 1353 (2015).

[24] Y. Saito, Y. Nakamura, M. S. Bahramy, Y. Kohama, J. Ye, Y. Kasahara, Y. Nakagawa, M. Onga, M. Tokunaga, T. Nojima, Y. Yanase, and Y. Iwasa, Nat. Phys. **12**, 144 (2016).

[25] X. Xi, Z. Wang, W. Zhao, J.-H. Park, K. T. Law, H. Berger, L. Forró, J. Shan, and K. F. Mak, Nat. Phys. **12**, 139 (2016).

[26] S. C. de la Barrera, M. R. Sinko, D. P. Gopalan, N. Sivadas, K. L. Seyler, K. Watanabe, T. Taniguchi, A. W. Tsen, X. Xu, D. Xiao, and B. M. Hunt, Nat. Commun. **9**, 1427 (2018).

[27] J. Cui, P. Li, J. Zhou, W.-Y. He, X. Huang, J. Yi, J. Fan, Z. Ji, X. Jing, F. Qu, Z. G. Cheng, C. Yang, L. Lu, K. Suenaga, J. Liu, K. T. Law, J. Lin, Z. Liu, and G. Liu, Nat. Commun. **10**, 2044 (2019).

[28] C. Wang, B. Lian, X. Guo, J. Mao, Z. Zhang, D. Zhang, B.-L. Gu, Y. Xu, and W. Duan, Phys. Rev. Lett. **123**, 126402 (2019).

[29] J. Falson, Y. Xu, M. Liao, Y. Zang, K. Zhu, C. Wang, Z. Zhang, H. Liu, W. Duan, K. He, H. Liu, J. H. Smet, D. Zhang, and Q.-K. Xue, Science **367**, 1454 (2020).

[30] A. Ptok, K. Rodríguez, and K. J. Kapcia, Phys. Rev. Mater. **2**, 024801 (2018).

[31] P. A. Frigeri, D. F. Agterberg, A. Koga, and M. Sigrist, Phys. Rev. Lett. **92**, 097001 (2004).

[32] J. A. Ouassou, T. D. Vethaak, and J. Linder, Phys. Rev. B **98**, 144509 (2018).

[33] Z.-J. Ying, M. Cuoco, C. Ortix, and P. Gentile, Phys. Rev. B **96**, 100506(R) (2017).

[34] G. Francica, M. Cuoco, and P. Gentile, Phys. Rev. B **101**, 094504 (2020).

[35] M. Smidman, M. B. Salamon, H. Q. Yuan, and D. F. Agterberg, Rep. Prog. Phys. **80**, 036501 (2017).

[36] V. Barzykin and L. P. Gor'kov, Phys. Rev. Lett. **89**, 227002 (2002).

[37] D. F. Agterberg and R. P. Kaur, Phys. Rev. B **75**, 064511 (2007).

[38] F. Loder, A. P. Kampf, and T. Kopp, J. Phys.: Condens. Matter **25**, 362201 (2013).

[39] O. Dimitrova and M. V. Feigel'man, Phys. Rev. B **76**, 014522 (2007).

[40] M. Houzet and J. S. Meyer, Phys. Rev. B **92**, 014509 (2015).

[41] D. Agterberg, Physica C: Supercond. **387**, 13 (2003).

[42] H. Jeffrey Gardner, A. Kumar, L. Yu, P. Xiong, M. P. Warusawithana, L. Wang, O. Vafek, and D. G. Schlom, Nat. Phys. **7**, 895 (2011).

[43] T. Champel and M. Eschrig, Phys. Rev. B **72**, 054523 (2005).

[44] F. S. Bergeret and I. V. Tokatly, Phys. Rev. B **89**, 134517 (2014).

[45] S. H. Jacobsen, J. A. Ouassou, and J. Linder, Phys. Rev. B **92**, 024510 (2015).

[46] X. Montiel and M. Eschrig, Phys. Rev. B **98**, 104513 (2018).

[47] A quantitative study of spin-charge conversion in Rashba superconductors is given in Ref. [53].

[48] See Supplemental Material at http://link.aps.org/supplemental/10.1103/PhysRevB.103.L020504 for the derivations and the details of the numerical method.

[49] D. Saint-James, G. Sarma, and E. Thomas, *Type II Superconductivity* (Pergamon Press, United Kingdom, 1969).

[50] The SOC in our model is weak ($\sim \xi^{-1}$). Therefore, we do not take the modulated order parameter into account, which is valid for strong SOC [39,40,42].

[51] L. A. B. Olde Olthof, X. Montiel, J. W. A. Robinson, and A. I. Buzdin, Phys. Rev. B **100**, 220505(R) (2019).

[52] G. C. Ménard, S. Guissart, C. Brun, R. T. Leriche, M. Trif, F. Debontridder, D. Demaille, D. Roditchev, P. Simon, and T. Cren, Nat. Commun. **8**, 2040 (2017).

[53] F. S. Bergeret and I. V. Tokatly, Phys. Rev. B **102**, 060506(R) (2020).

[54] M. Eschrig, Rep. Prog. Phys. **78**, 104501 (2015).

[55] We consider films with lateral dimensions down to $L \sim \xi$, while the thickness is $d \sim \xi$. We expect all modifications to the superconducting order to take place in plane, since there is no inhomogeneity in the system along z. This is valid when neglecting orbital effects and proximity effects.

[56] K. Premasiri, S. K. Radha, S. Sucharitakul, U. R. Kumar, R. Sankar, F.-C. Chou, Y.-T. Chen, and X. P. A. Gao, Nano Lett. **18**, 4403 (2018).

[57] A. M. Afzal, M. F. Khan, G. Nazir, G. Dastgeer, S. Aftab, I. Akhtar, Y. Seo, and J. Eom, Sci. Rep. **8**, 3412 (2018).